Title
Restoration of Hearing in the VGLUT3 Knockout Mouse Using Virally Mediated Gene Therapy

Journal
Neuron, 75(2)

ISSN
0896-6273

Authors
Akil, Omar
Seal, Rebecca P
Burke, Kevin
et al.

Publication Date
2012-07-01

DOI
10.1016/j.neuron.2012.05.019

Peer reviewed

Published in final edited form as:
Neuron. 2012 July 26; 75(2): 283–293. doi:10.1016/j.neuron.2012.05.019.

Restoration of Hearing in the VGLUT3 Knockout Mouse Using Virally-Mediated Gene Therapy

Omar Akil,
Department of Otolaryngology- Head & Neck Surgery, University of California San Francisco, San Francisco, CA, 94143-0449. Phone: 415-476-0728. oakil@ohns.ucsf.edu

Rebecca P. Seal,
Department of Neurology- University of Pittsburgh, Pittsburgh, PA 15213-3301. Phone: 412-624-5183. rpseal@pitt.edu

Kevin Burke,
Department of Otolaryngology- Head & Neck Surgery, University of California San Francisco, San Francisco, CA, 94143-0449. Phone: 415-476-0728. kburke@ohns.ucsf.edu

Chuansong Wang,
Comprehensive Cancer Center, The Ohio State University, Columbus, Ohio. Phone: 614-247-4351

Aurash Alemi,
Department of Otolaryngology- Head & Neck Surgery, University of California San Francisco, San Francisco, CA, 94143-0449. Phone: 415-476-0728. AAlemi@ohns.ucsf.edu

Matthew During,
Comprehensive Cancer Center, The Ohio State University, Columbus, Ohio. Phone: 614-247-4351. Matthew.During@osumc.edu

Robert H. Edwards, and
Department of Neurology, University of California San Francisco, San Francisco, CA, 94143-2140. Phone: 415-502-5687. robert.edwards@ucsf.edu

Lawrence R. Lustig

Summary

Mice lacking the vesicular glutamate transporter-3 (VGLUT3) are congenitally deaf due to loss of glutamate release at the inner hair cell afferent synapse. Cochlear delivery of VGLUT3 using adeno-associated virus-1 (AAV1) leads to transgene expression in only inner hair cells (IHC), despite broader viral uptake. Within two weeks of AAV1-VGLUT3 delivery, acoustic brainstem response (ABR) thresholds normalize, along with partial rescue of the startle response. Lastly, we demonstrate partial reversal of the morphologic changes seen within the afferent IHC ribbon synapse. These findings represent the first successful restoration of hearing by gene replacement in mice, which is an important step towards gene therapy of human deafness.

Senior Author Correspondence: Lawrence R. Lustig, MD, Director, UCSF Hair Cell Physiology Lab, Department of Otolaryngology-Head & Neck Surgery, University of California San Francisco, U401, Box 0449, San Francisco, CA 94143-0449, PH: 415-476-0728, Fax: 415-476-0708, llustig@ohns.ucsf.edu.

Introduction

Hearing loss is one of the most common human sensory deficits, with congenital hearing loss occurring in approximately 1.5 in 1000 children (Smith et al., 2005). Of these, about half are attributed to a genetic basis (Di Domenico et al., 2010). While our understanding of the causes of genetic hearing loss has advanced tremendously over the past 30 years (Petersen and Willems, 2006), treatments have advanced little over this same time period, and currently consist of hearing amplification for mild to severe losses, and cochlear implantation for severe to profound losses (Kral and O'Donoghue, 2010). Though cochlear implantation has profoundly influenced our treatment of children with congenital deafness, there are still significant limitations in function with an implant, and these results cannot compare to native hearing (Kral and O'Donoghue, 2010). Thus there remains intense interest in restoring normal organ of Corti function through techniques such as hair cell regeneration and gene therapy (Di Domenico et al., 2010). To date, a majority of the research in this arena has focused on cochlear hair cell regeneration, applicable to the most common forms of hearing loss including presbycusis, noise-damage, infection, and ototoxicity. Several studies have now demonstrated regeneration of hair cells in injured mice cochlea, and improvement of both hearing and balance with virally-mediated delivery of *Math1* (Baker et al., 2009; Husseman and Raphael, 2009; Izumikawa et al., 2008; Kawamoto et al., 2003; Praetorius et al., 2009; Staecker et al., 2007). While these efforts in wild-type animals are quite important, they still do not address the problem of an underlying causative genetic mutation. In such a scenario, even successfully regenerated hair cells will still be subject to the innate genetic mutation that led to hair cell loss in the first place. To date, efforts to restore hearing in this type of hearing loss with gene therapy have been met with limited success (Maeda et al., 2009), and no study has reported the reversal of deafness in an animal model of genetic deafness.

Previous reports have described a mouse model of hereditary deafness, which occurs as a result of a null mutation in the gene coding for the vesicular glutamate transporter 3 (VGLUT3) (Obholzer et al., 2008; Ruel et al., 2008; Seal et al., 2008). Synaptic transmission mediated by glutamate requires transport of the excitatory amino acid into secretory vesicles by a family of three vesicular glutamate transporters (Fremeau et al., 2004; Takamori et al., 2002). We previously demonstrated that inner hair cells of the cochlea express VGLUT3 and that mice lacking this transporter are congenitally deaf (Seal et al., 2008). Hearing loss in these mice is due to the elimination of glutamate release by inner hair cells and hence to the loss of synaptic transmission at the IHC-afferent nerve synapse. Subsequent studies have shown that a missense mutation in the human gene SLC17A8, which encodes VGLUT3, might underlie the progressive high frequency hearing loss seen in autosomal dominant DFNA25 (Ruel et al., 2008). Here we report the successful restoration of hearing in the VGLUT3 KO mouse using virally-mediated gene delivery.

Results

AAV1-VGLUT3 transfection results in localized expression in inner hair cells

Our first goal was to determine the extent of transfection with the adeno-associated virus type 1 (AAV1) within the cochlea. Using an AAV1-GFP construct, there appeared to be labeling of a variety of cell types within the cochlea, including the inner hair cells and supporting cells using an anti-GFP antibody (Figure 1A), in a pattern similarly described by other investigators (Jero et al., 2001; Konishi et al., 2008). Subsequently, virus containing the VGLUT3 gene (AAV1-VGLUT3) was microinjected into the cochlea using two different techniques; initially via an apical cochleostomy (CO), and subsequently by direct injection through the round window membrane (RWM) (Figure 1B–E). Following delivery, RT-PCR of inner ear tissue (Figure 1C) demonstrated strong VGLUT3 mRNA expression in

the rescued whole cochlea, organ of Corti, stria vascularis, vestibular neuroepithelium, and very weakly in the spiral ganglion. Non-injected cochleas of knock-outs do not demonstrate VGLUT3 expression as noted (Figure 1C, KO −/+RT). In contrast, under immunofluorescence, inner hair cells were the only cells labeled with anti-VGLUT3 antibody (Figure 1B).

To determine the dose-dependence of VGLUT3 expression in the IHCs, we injected either 0.6 μl or 1μl of AAV1-VGLUT3 (2.3×10^{13} virus genomes (vg)/ml) into the cochlea (Figure 1D–E). Microinjecting 1μl of virus resulted in 100% of IHCs labeled with anti-VGLUT3 antibody; in contrast, microinjecting 0.6μl resulted in only ~ 40% of IHCs labeled by the antibody.

We next sought to determine if earlier viral delivery would result in more robust VGLUT3 expression (Figures 1D–E, 2). As shown, delivery of virus via the RWM at post-natal day 10 (P10) results in ~40% of the IHCs expressing VGLUT3 (Figures 1D–E, 2), whereas similar doses (0.6 μl) of virus injected at the P1-3 results in 100% of IHC transfected in all animals (Figures 1D–E, 2).

Delivery of AAV1-VGLUT3 restores normal ABR and CAP thresholds within 14 days

After verifying successful transgene expression within the IHC without significant organ of Corti injury, we next sought to determine whether the reintroduction of VGLUT3 would lead to measureable hearing recovery (Figure 3). In these studies only 0.6μl of AAV1-VGLUT3 was delivered at P10-12. Acoustic brainstem response (ABR) thresholds were first measurable within 7 days following viral delivery, with near normalization of thresholds to wild-type (WT) levels within 2 weeks (P24-26) (Figure 3A–C). Initially a cochleostomy (CO) technique was used for viral delivery. However, this method restored hearing in only ~17% of animals (n=5 out of 30 animals attempted), presumably because it was more technically challenging and due to the trauma of the approach (*see discussion*). As a result, the method was subsequently changed to a round window membrane (RWM) delivery, which resulted in hearing restoration in 100% of mice (n=19 out of 19 mice). The time course of hearing recovery was similar for the CO (when successful in 17%) and the RWM delivery techniques (100% of mice). Compound action potentials (CAPs) were also restored within 7–14 days of viral delivery (Figure 3A). Since the loss of VGLUT3 affects only glutamate release at the IHC synapse (Ruel et al., 2008; Seal et al., 2008), restoration of normal ABRs and CAPs also implies restoration of synaptic function. We also compared the longevity of hearing recovery, defined as the period of time between onset of hearing recovery and when ABR thresholds become elevated > 10db above WT levels, between the CO and RWM methods (Figure 3D). In both groups, all rescued KO mice maintained hearing for at least 7 weeks. At 28 weeks post-delivery 40% of the mice who achieved successful CO delivery still had hearing within 10db of WT mice (n=2/5), while only 5% of the RWM mice had the same level of hearing (n=1/19). Interestingly, some rescued mice in each group, CO and RWM, maintained normal ABR thresholds up to 1.5 years. The number of animals for each rescued group at each time point, within 10db of WT thresholds, is described in the legend of figure 3D.

We subsequently measured hearing recovery in mice injected via the RWM at P1-3 (Figure 3D). Due to the small size of the cochlea, only 0.6 μl of virus could be delivered at this time point. However, 100% of mice recovered normal ABR thresholds by P14 (n=19 mice). Five mice were followed for 9 months and still maintained normal ABR thresholds at this later time point. Earlier delivery thus not only appears to be more efficient (100% of animals recover hearing), but also leads to greater longevity of hearing recovery.

Bilateral AAV1-VGLUT3 rescue results in a larger recovery of behavioral and electrical measures of hearing

For an additional assay of hearing recovery we studied the startle response at approximately 3 weeks following viral delivery (Figure 4). In these experiments, the AAV1-VGLUT3 delivery was done via the RWM at age P10-12. As expected, VGLUT3 KO mice show no startle response due to the absence of hearing. When hearing was rescued in one ear ("Unilat", Figure 4A), at the loudest presentation level of 120dB, the startle response improved to 8% of normal, while if both ears were rescued ("Bilat", Figure 4A) the startle response increased to 33% of normal, both measures being statistically different than the KO response. Interestingly, similar amplitude growth was observed with ABR wave I amplitudes when both ears, as opposed to a single ear, were rescued (Figure 4B). ABR wave I latency was also studied (Figure 4C), and while there appeared to be a trend for reduced latency in the unilateral rescued mice, the differences between unilateral- and bilateral-rescued and WT mice were not significant. Thus, while ABR thresholds can be brought to normal, "behavioral" thresholds and ABR amplitudes can be improved, but not normalized to the WT level with this rescue technique.

AAV1-VGLUT3 rescue partially restores synaptic morphology, but not spiral ganglion cell counts in the knockout mouse

As we previously demonstrated (Seal et al., 2008), at P21 VGLUT3 KO mice show a 10–18% decrease in spiral ganglion (SG) neurons compared to WT mice. This decrease was still observed in the AAV1-VGLUT3 rescued mice (RWM delivery at P10-12) at P21 (Figure 5A). Further, rescued mice showed no significant differences in spiral ganglion cell size as compared to KO mice (Figure 5B), though both were significantly less than WT mice. To determine whether long-term hearing would reverse this trend, counts were also taken at P5months, but again, no significant differences in SG counts or cell size were seen in the KO vs. rescued mice at this later time point (*data not shown*). Subsequently, spiral ganglion cell counts were also undertaken in mice that underwent virus delivery at P1-3. However, despite a robust IHC transfection and early hearing recovery (see Figures 1D–E, 2), again, no differences in SG cell counts were noted between KO and rescued mice (*data not shown*). Additionally, histology (Figure 5C) documents no obvious cochlear trauma as a result of viral delivery in the rescued mice, as evidenced by normally appearing organ of Corti structures with preservation of inner- and outer-hair cells, supporting cells, spiral ganglion neurons (though similarly reduced in number as non-rescued mice) and the stria vascularis (*data not shown*).

As originally reported, VGLUT3 KO mice demonstrate abnormally thin, elongated ribbons in IHC synapses, though the number of synaptic vesicles tethered to ribbons or docked at the plasma membrane were normal (Seal et al., 2008). We thus sought to determine if these morphologic abnormalities could be reversed with hearing rescue. As shown (Figure 6, Table 1), in the rescued mice, ribbon synapses are normal in appearance, taking on a more rounded shape similar to the WT, while the non-rescued mice continue to demonstrate abnormally thin and elongated ribbons. The rescued mice also displayed a significantly larger number of synaptic vesicles associated with the ribbon (19 rescued vs. 14 WT, $p=0.02$) (Table 1). Interestingly, within individual hair cells, the synaptic vesicles themselves demonstrated a mixture of elongated and circular morphology, as opposed to all circular in the WT and all elongated in the KO mice. However, when analyzing the average number of docked synaptic vesicles at a ribbon synapse, rescued animals did not show a significant difference between either the WT or KO mice (Table 1). While these results demonstrate only a partial reversal of the synaptic changes seen in the KO mouse ribbon synapse, it is enough to recover ABR thresholds to the WT levels in the rescued KO mice.

Discussion

These studies document the successful rescue of the deafness phenotype in a mouse model of inherited deafness. With viral delivery of VGLUT3 at P10-12 in the KO mouse, ABR thresholds normalize within 7–14 days, and remain in this range for at least 7 weeks, with 2 mice maintaining auditory thresholds for as long as a year and a half in this current study. Earlier delivery, at P1-3, results in an even more robust IHC transfection and long-lived hearing recovery in this mouse model.

One unexpected result from these investigations was the differential finding of more widespread expression of GFP protein following AAV1-GFP transfection as compared to isolated VGLUT3 expression restricted to the IHC following AAV1-VGLUT3 transfection (Figure 1A–C, 2). RT-PCR results demonstrate that following AAV1-VGLUT3 delivery, there is also more widespread VGLUT3 mRNA transcription than in just IHCs (Figure 1C). These results suggest that there is a post-transcriptional regulatory mechanism acting on VGLUT3 mRNA which leads to selective expression of the protein only within IHCs. Several types of post-transcriptional regulation have been described within the cochlea, and whether this specific mechanism involves microRNA inactivation (Elkan-Miller et al., 2011), transcription factor regulation (Masuda et al., 2011) or another process remains to be determined. Such a mechanism, if appropriately elucidated and exploited, could theoretically allow the expression (or conversely suppression) of a number of different proteins within the inner ear to alter function in pursuit of hearing preservation.

Another interesting finding was the variable success with the cochleostomy (CO) as compared to the round window membrane (RWM) delivery technique. As noted, we initially started with an apical CO delivery method, but abandoned it due to the low success rate of hearing restoration (17% of animals). Subsequently, we changed to a RWM delivery technique for several reasons; this would be the most likely method of delivery in any future human studies, and it was less likely to be traumatic, as evidenced by a number of recent human studies looking at hearing preservation with round window insertion of cochlear implants (von Ilberg et al., 2011). In fact, the change in technique resulted in hearing restoration in 100% of animals attempted. We believe the likely difference in success between the two techniques relates to the degree of trauma induced by each method. With a cochleostomy, a separate hole into the scala through bone must be created which by its nature is traumatic, despite our best efforts to minimize trauma. In contrast, a RWM injection simply involves piercing the membrane and sealing it with fascia following viral delivery. However, histologically we were unable to see any obvious differences between the ears of animals with and without hearing rescue in the cochleostomy group (data not shown) and there may be other reasons for the variable success between the two techniques. Further, we noted that even earlier delivery via the RWM at P1-3, as opposed to P10-12, resulted in hearing recovery that was more consistently long-lived, with all mice followed out through 9 months showing ongoing normal ABR thresholds (Figure 3D).

Transgene expression with AAV1 should theoretically last for a year or longer (Henckaerts and Linden, 2010). However it is not entirely clear why there is a variable loss of hearing after 7 weeks, regardless of delivery technique at the later P10-12 delivery time point (Figure 3D). We analyzed individual cochleae but did not see histologic evidence of active inflammation in those animals that lost hearing and IHCs still expressing VGLUT3 protein. Further, spiral ganglion counts did not significantly differ in animals with and without hearing. One possibility could be due to the trauma of viral delivery, with gradual reopening of the delivery site (RWM or cochleostomy) leading to a perilymphatic leak with resulting hearing loss. Such a lesion might not be detectable on histology. Another possible explanation may be due to transgene inactivation, by a hypothetical mechanism such as

microRNA inactivation or methylation. Clearly if one hopes to consistently achieve long-term transgene expression within the ear, which will be critical for application of this technique in humans, this variable will need to be better understood and controlled, particularly at later ages of delivery.

It is interesting to note that the lower dose of virus used for most of the studies performed (0.6μl), delivered at P10-12, caused VGLUT3 expression in only ~40% of IHCs (Figure 1D–E), and yet this was enough to restore ABR thresholds to WT levels for click responses, and near normal for pure tone thresholds (Figure 3A–C). Similar results have been documented in other models of hearing recovery following noise-exposure (Kujawa and Liberman, 2009; Lin et al., 2011), where even “reversible” noise exposure with recovery of auditory thresholds leads to long-term afferent nerve terminal degeneration while retaining ‘normal’ auditory thresholds. Similar findings with regard to the discrepancy of ABR threshold and amplitudes have also been shown from mutant mice lacking synaptic ribbons (Buran et al., 2010). However, correlative studies in human temporal bones suggest that cochlear implants in humans can still function very effectively despite significant spiral ganglion neuron loss, allowing for meaningful speech and sound transmission (Gassner et al., 2005; Khan et al., 2005). Thus, complete normalization of all cellular abnormalities may ultimately not be required for the technique to be successful in humans, though this should remain a goal for animal studies going forward.

The KO mice develop an unusual appearing ribbon that is thin and elongated, as noted here and previously (Seal et al., 2008). A similar ribbon morphologic pattern, flat and plate-like, is seen in the Otoferlin KO mouse (Roux et al., 2006). As Otoferlin is also critical in glutamate release at the IHC synapse, this implies that lack of physiologic activity of the synapse results such a flat ribbon appearance. In the rescued mice, while the ribbon itself appeared normal, we did still see a mixture of elongated and circular vesicles within the transfected IHCs, as opposed to all circular in the WT and all elongated in the KO mice, implying that there may still be differences in transmitter release in the rescued vs. WT mice.

Another interesting finding with regard to the ribbon synapse was the larger numbers of synaptic vesicles that were associated with the ribbon seen in the rescued mice, as well as the mixture of elongated and circular vesicles observed. The data shows that much larger quantities of VGLUT3 mRNA are being produced in the rescued as compared to the WT mice (Figure 1C RT-PCR data), and suggests, though does not prove, an association between increased mRNA levels and vesicle number. We believe that circular vesicles represent properly packaged vesicles, while the elongated vesicles are improperly packaged vesicles. Perhaps continuous production of VGLUT3 by the constitutive CBA promoter driving transfected VGLUT3 production prevents the IHC from properly packaging the vesicles at a normal rate, leading to a higher number as well as a mixture of regular and irregular-appearing vesicles. Another possibility is that the incomplete transfection rate of IHCs (40% of IHCs labeled at the doses used for these morphology studies), led to the heterogeneity of the ribbon morphology seen.

The observed growth on behavioral and electrical measures seen with bilateral, as opposed to unilateral rescue (RWM delivery at P10-12 (Figure 4) was an unexpected finding. While none of the animals had complete normalization of ABR amplitude and startle-response levels, the amplitude growth does imply that bilateral input increases the auditory response centrally. An analogous phenomenon is seen with ‘binaural summation’, and clinically in patients who wear two hearing aids as opposed to one and report lower levels of amplification required (Noble, 2010; Steven Colburn et al., 2006) and suggests that the response seen in these studies is physiologic. Recent studies have localized VGLUT3 to

various structures in the brainstem, including cochlear nucleus (Fyk-Kolodziej et al., 2011) as well as the LSO and MNTB (Lee et al., 2011). It is certainly possible that deficits within auditory brainstem signal pathways could be contributing to the inability to restore the startle response to WT levels.

The failure of the technique to reverse the spiral ganglion cell loss seen in the VGLUT3 KO mice when delivered at P10-12 is not surprising (Figure 5), given that hair cell activity and afferent stimulation can provide a trophic effect on SG survival. This is likely at least partly due to the fact that virus was delivered at ~P10 with subsequent ABR thresholds recovery at ~P17-24, after spiral ganglion neuronal degradation has begun (Seal et al., 2008). This also implies that in order for SG neurons to be preserved at normal levels, intervention would likely have to occur earlier. Further, with only ~40% of IHCs expressing VGLUT3 (using the lower concentration of virus, delivered at P10-12), there are still many spiral ganglion neurons not receiving afferent input, which also likely impacts this result as well. We were thus surprised that even earlier delivery of virus, at P1-3, which resulted in relatively early onset of hearing, measureable by P14, with 100% of IHC expressing VGLUT3, also did not lead to restoration of SG cell counts to WT levels. Perhaps there are *in utero* factors that also help maintain SG numbers, or even a small delay in hearing onset can lead to SG loss.

Lastly, while the mutant mouse in the current study and the hearing loss described in patients with DFNA25 are both due to mutations in the gene coding for VGLUT3, the comparison may not be straightforward. First, it is not certain that the missense mutation described in SLC17A8 is the cause of the hearing loss seen in DFNA25, though a strong correlation was observed (Ruel et al., 2008). Second, the null mutation studied in these experiments would represent a much more severe phenotype than the missense mutation described as potentially causative for DNFA25. Thus whether this technique could ultimately be beneficial to patients with DFNA25 remains unclear. Despite these differences, as the first study to document restoration of normal ABR levels in such a null-mutant model, it nonetheless represents an important initial step for the potential treatment of inherited deafness.

Experimental Procedures

Animals

VGLUT3 null mutant mice were generated as described in a C57 (Seal et al., 2008) strain then backcrossed with FVB mice (> 7 generations) to obtain a homogeneous genetic background. P1 – 12 mice were used for AAV1-VGLUT3 delivery. All procedures and animal handling complied with NIH ethics guidelines, and approved protocol requirements at the University of California, San Francisco (IACUC).

All surgical procedures were done in a clean, dedicated space. Instruments were thoroughly cleaned with 70% ETOH and autoclaved prior surgery. Surgery was carried out under a Leica MZ95 dissecting scope and animals were situated with neck extended over solid support. Mice were anesthetized by intraperitoneal injection of a mixture of Ketamine hydrochloride (Ketaset, 100 mg/kg), Xylazine hydrochloride (Xyla-ject, 10 mg/kg) and Acepromazine (2mg/kg) and boosted with one fifth the original dose as required. Depth of anesthesia was continuously checked by deep tissue response to toe pinch. Body temperature was maintained with a heating pad and monitored with a rectal probe throughout procedures. Preoperatively and every 24hrs postoperatively animals were given subcutaneous Carprofen analgesia (2mg/kg) to manage inflammation and pain. Animals were closely monitored for signs of distress and abnormal weight loss postoperatively.

AAV1-VGLUT3 Viral Construct

Mouse *VGLUT3* cDNA was sub-cloned into the multiple cloning site of vector AM/CBA-WPRE-BGH (kindly provided by R. Palmiter). Human embryonic kidney 293 cells were co-transfected with three plasmids—AAV-mVGLUT3 plasmid, appropriate helper plasmid encoding rep and AAV1 cap genes, and adenoviral helper pF Δ6—using standard CaPO4 transfection. Cells were harvested 60 hours following transfection, cell pellets lysed with sodium deoxycholate and AAV vectors purified from the cell lysate by ultracentrifugation through an iodixanol density gradient, then concentrated and dialyzed against phosphate-buffered saline (PBS), as previously described (Cao et al., 2009; Cao et al., 2010; Lawlor et al., 2009). Vectors were titered using real-time PCR (ABI Prism 7700; Applied Biosystems, Foster City, CA), and purity of vector stocks was confirmed by running a 10 μl sample on sodium dodecyl sulfate polyacrylamide gel electrophoresis and staining with Coomassie blue.

SURGICAL PROCEDURES

Round Window Membrane (RWM) Injection—Animals were anesthetized, the left ear was approached via a dorsal incision as described by Duan *et al* (Duan et al., 2004). A small hole was made in the bulla with an 18g needle and expanded as necessary with forceps and the round window membrane (RWM) was identified. The RWM was gently punctured with a borosilicate capillary pipette and remained in place until efflux stabilized. A fixed volume of AAV1- VGLUT3 (0.6 μl or 1.0 μl of a 2.3 10^{13} virus genomes/ml) previously drawn into the fine pipette was gently injected through RWM over 1–2 minutes. After pulling out the pipette, the RW niche was quickly sealed with fascia and adipose tissue. The bulla was sealed with dental cement (Dentemp, Majestic Drug Company, South Fallsburg, NY) and the wound was sutured in layers with a 5-0 absorbable chromic suture (Ethicon, New Jersey).

Cochleostomy delivery—The right ear was approached via ventral, paramedian incision in the neck as described by Jero et al(Jero et al., 2001). The injection method was similar to the RWM except that the hole in bulla was made slightly more anterior and larger, to directly approach the space above the stapedial artery. Injection of virus was made into the apical turn. Using a 0.5 mm drill pit to thin gently the bone of the otic capsule where the stria vascularis could be slightly visualized as a brownish stripe. Once enough bone was shaved a slight fluid interface became visible, 0.6 μl VGLUT3-AAV1 (2.3 10^{13} virus genomes/ml) was pipetted into the hole over a period of 1–2 minutes. Following application the hole in the cochlea was sealed with a small amount of bone wax. After dried a small amount of sterile tissue glue is applied to the bone wax and the bulla was sealed and the wound was sutured as described above.

AUDITORY TESTING

Acoustic startle response testing—Acoustic startle responses of VGLUT3 KO (n = 5), WT littermate (n = 5), rescued VGLUT3 KO one ear (n = 5) and rescued VGLUT3 KO bilateral (n=5) mice were measured as previously described (Seal et al., 2008). In brief in darkened startle chambers (SR-LAB hardware and software, San Diego Instruments), piezoelectric sensors located under the chambers detect and measure the peak startle response. Mice were acclimatized to the startle chambers by presentation of a 70 dB white noise for 5 min and then exposed to sound intensities of 100 dB, 110 dB and 120 dB (each with a 0 ms rise time, 40 ms plateau, 0 ms fall time), presented in pseudorandom order with intersound intervals of 10–50 s. Each run was repeated eight times. Average peak startle amplitude at each sound level was calculated from eight runs. Final results were calculated as a percentage of WT mice at the 120 dB presentation level. Statistical significance

between measures was determined using a student‘s T-test with significance defines as $p<0.05$.

Auditory brainstem response (ABR) recording—Sound were presented and ABRs were tested in a free field conditions as previously described in a sound-proofed chamber (Akil et al., 2006; Fremeau et al., 2004). ABR thresholds were determined postoperative at varying time-points, as early as 4 days following viral delivery for P10-12 mice. The mean value of thresholds checked by visual inspection and computer analysis was defined as ABR hearing threshold for click and 8, 16 and 32 KHz tones stimulus.

Compound action potential (CAP) recording—For the CAP recording, a ventral surgical approach (Jero et al., 2001) was used to expose the right cochlea 7–14 days following AAV1-VGLUT3 delivery to the inner ear of the P10-12 mice, including KO (n=5), rescued KO (n=8) and WT littermates (n =5). A fine Teflon-coated silver wire recording electrode was placed in the round window niche, and the ground electrode was placed in the soft tissue of the neck. The sound stimulus was generated with Tucker-Davis System II hardware and software (Tucker-Davis Technologies, Alachua, FL, USA).

IMMUNOFLUORESCENCE

Immunofluorescence studies were conducted similarly for whole-mount and cochlear sections with the following differences:

Cochlear whole mount—Mice cochleae were perfused with 4% PFA in 0.1 M PBS (phosphate buffered saline), pH 7.4, and incubated in the fixative for 2 hours at 4°C. The cochleae were subsequently rinsed with PBS three times for 10 min, and then decalcified with 5% EDTA in 0.1 M PBS. The otic capsule, the lateral wall, tectorial membrane, and Reissner‘s membrane were removed in that order. The remaining organ of Corti was further dissected into a surface preparation (microdissected into individual turns) then pre-incubated for 1 hr in PBS containing 0.25% Triton X-100 and 5% normal goat serum (blocking buffer). The whole mount was then incubated with rabbit anti- myosin VIIa antibody (a hair cell specific marker) (Proteus Biosciences, INC Cat # 25-6790) at a dilution of 1:50 in blocking buffer and Guinea pig anti-VGLUT3 antibody (a gift from Dr.Robert Edwards, Dept. of Neurology, UCSF) at 1:5000. After an overnight incubation at 4°C, the cochlear whole mount was rinsed twice for 10 min with PBS and then incubated for 2 h in goat anti-rabbit IgG conjugated to Cy2 and goat anti guinea pig IgG conjugated to Cy3 diluted to 1:4000 in PBS. Specimens were next rinsed in PBS twice for 10 min, and mounted on glass slides in a mounting solution containing DAPI (nucleus stain) and observed under an Olympus microscope with confocal immunofluorescence. For inner hair cells counts the cochlear whole mounts were visualized under a microscope equipped with epifluorescence, using a 40X objective. To quantify the number of IHC transfected with AAV1-VGLUT3 specimens were labeled with anti-VGLUT3 antibody, and IHCs were manually counted in the cochlear whole mount and in the base, mid-turn and apex. . For GFP labeling, surface preparation (cochlea whole mount) were incubated with a rabbit anti GFP antibody (Invitrogen # A11122) at 1:250. After an overnight incubation at 4°C, the cochlea sections were rinsed twice for 10 min with PBS and then incubated for 2 h in goat anti-rabbit IgG conjugated to Cy2 diluted to 1:4000 in PBS. Then rinsed in PBS twice for 10 min, and mounted on glass slides in a mounting solution containing DAPI and observed under an Olympus microscope with confocal immunofluorescence.

Cochlear sections—Mice were anesthetized and their cochleae were isolated, dissected, perfused through oval and round windows by 2% paraformaldehyde in 0.1 M PB at pH 7.4, and incubated in the same fixative for 2 h. After fixation, the cochleae were rinsed with PBS

and immersed in 5% EDTA in 0.1M PB for decalcification. When the cochleae were completely decalcified, they were incubated overnight in 30% sucrose for cryoprotection. The cochleae then were embedded in OCT Tissue Tek Compound (Miles Scientific). Tissues were cryosectioned at 10–12 μm thickness, mounted on Superfrost microscope slides (Erie Scientific), and stored at −20°C until use. Sections were then double labeled as described above (see cochlear whole mount). Slides were then mounted in a 1:1 mixture of PBS and glycerol before being coverslipped. Slides treated with the same technique but without incubation with the primary antibody were used as controls

HISTOLOGY

Light microscopy—Cochleae were isolated from deeply anesthetized WT, VGLUT3 KO and rescued KO mice, perfused through oval and round windows with 2.5% paraformaldehyde 1.5% glutaraldehyde in 0.1M PB at pH 7.4 and incubated overnight at 4°C with slow agitation in fixative. The cochleae were rinsed with 0.1 M PB and post fixed in 1% osmium tetroxide and 1.5% potassium ferricyanide (for improved contrast) for 2 h. The cochleae subsequently were immersed in 5% EDTA (0.2 M). The decalcified cochlea were dehydrated in ethanol and propylene oxide and embedded in Araldite 502 resin (Electron Microscopy Sciences, Fort Washington, PA) and sectioned at 5μm. After sections were stained with Toluidine Blue, they were mounted in Permount (Fisher Scientific, Houston, TX) on microscope slides.

Electron microscopy—Electron microscopy was performed as previously described (Akil et al., 2006) on broken serial thin sections of the synaptic region of the IHCs which were cut in a horizontal plane parallel to the basilar membrane. In this study the cochleae were all handled and cut exactly the same and the same protocol and orientation for the WT, KO and rescued KO were applied when examining and visualizing the synaptic ribbons and vesicles. The morphological assessment of ribbons and vesicles was performed as described by Roux et al (Roux et al., 2006) using 50–61 IHCs and 17–20 different IHCs ribbons synapse from three WT and three KO and three rescued KO mice. Sections were stained with uranyl acetate and lead citrate and examined under a 60 kV in a JEOL-JEM 100S transmission electron microscope. The number of vesicles tethered to the ribbon included all the vesicles within 30nm of the ribbon. All the vesicles clearly located immediately below the ribbon were considered to be docked in our 2D estimation.

Spiral ganglion cell counts—Spiral ganglion cell numerical density assessment was calculated as described by Leake et al (Leake et al., 2011) to accurately estimate the number of nuclei in a given volume of tissue. For this analysis 3 sets of 3 serial sections (5 μm thickness, were collected from the base, mid-turn and the apex of 4 WT, 3 KO and 4 rescued KO cochlea. Adjacent serial sections were compared, and new nuclei of spiral ganglion neurons that appear in the second section were counted. Statistical differences were measured using a student‘s T-test.

RT- PCR of the Cochlea

Cochlea from WT, VGLUT3 KO and rescued KO were dissected. The total RNA was extracted from the whole cochlea, organ of Coti + stria vascularis, spiral ganglion and vestibular epithelium (Trizol™, Invitrogen Corp) and reverse transcribed with superscript II RNase H− (Invitrogen) for 50 min at 42°C, using oligodT primers (Akil et al., 2006). Reactions without the reverse transcriptase enzyme (−RT) were performed as control. Two microliters of RT reaction product was used for subsequent polymerase chain reaction (PCR; Taq DNA Polymerase, Invitrogen) of 35 cycles using the following parameters: 94°C for 30 s, 60°C for 45 s, 72°C for 1 min, followed by a final extension of 72°C for 10 min and storage at 4°C. Primers were designed to amplify a unique sequence of VGLUT3 isoform of

759 bp. The PCR primers that were used for mouse include: VGLUT3 (Genbank accession number AF510321.1: forward-(gctggaccttctatttgctctta) and reverse- (tctggtaggataatggctcctc). Analysis of each PCR sample was then performed on 2% agarose gels containing 0.5 μg/ml ethidium bromide. Gels were visualized using a digital Camera and image processing system (Kodak, Rochester NY, USA). Candidate bands were cut out and the DNA was extracted (Qiaquick gel extraction kit, Qiagen) and sequenced (Elim Biopharmaceuticals, Inc. Hayward, CA, USA). The PCR product was then compared directly to the full VGLUT3 sequence for identity.

Acknowledgments

We thank Dr. Diana Bautista and Dr. Makoto Tsunozaki (UC Berkeley) for critical advice and the use of their startle response chamber.

The authors would like to acknowledge the financial support provided by Hearing Research Inc.

Bibliography

Akil O, Chang J, Hiel H, Kong JH, Yi E, Glowatzki E, Lustig LR. Progressive deafness and altered cochlear innervation in knock-out mice lacking prosaposin. J Neurosci. 2006; 26:13076–13088. [PubMed: 17167097]

Baker K, Brough DE, Staecker H. Repair of the vestibular system via adenovector delivery of Atoh1: a potential treatment for balance disorders. Adv Otorhinolaryngol. 2009; 66:52–63. [PubMed: 19494572]

Buran BN, Strenzke N, Neef A, Gundelfinger ED, Moser T, Liberman MC. Onset coding is degraded in auditory nerve fibers from mutant mice lacking synaptic ribbons. The Journal of neuroscience : the official journal of the Society for Neuroscience. 2010; 30:7587–7597. [PubMed: 20519533]

Cao L, Lin EJ, Cahill MC, Wang C, Liu X, During MJ. Molecular therapy of obesity and diabetes by a physiological autoregulatory approach. Nat Med. 2009; 15:447–454. [PubMed: 19270710]

Cao L, Liu X, Lin EJ, Wang C, Choi EY, Riban V, Lin B, During MJ. Environmental and genetic activation of a brain-adipocyte BDNF/leptin axis causes cancer remission and inhibition. Cell. 2010; 142:52–64. [PubMed: 20603014]

Di Domenico M, Ricciardi C, Martone T, Mazzarella N, Cassandro C, Chiarella G, D'Angelo L, Cassandro E. Towards gene therapy for deafness. J Cell Physiol. 2010

Duan M, Venail F, Spencer N, Mezzina M. Treatment of peripheral sensorineural hearing loss: gene therapy. Gene Ther. 2004; 11(Suppl 1):S51–S56. [PubMed: 15454957]

Elkan-Miller T, Ulitsky I, Hertzano R, Rudnicki A, Dror AA, Lenz DR, Elkon R, Irmler M, Beckers J, Shamir R, et al. Integration of transcriptomics, proteomics, and microRNA analyses reveals novel microRNA regulation of targets in the mammalian inner ear. PLoS One. 2011; 6:e18195. [PubMed: 21483685]

Fremeau RT Jr, Kam K, Qureshi T, Johnson J, Copenhagen DR, Storm-Mathisen J, Chaudhry FA, Nicoll RA, Edwards RH. Vesicular glutamate transporters 1 and 2 target to functionally distinct synaptic release sites. Science. 2004; 304:1815–1819. [PubMed: 15118123]

Fyk-Kolodziej B, Shimano T, Gong TW, Holt AG. Vesicular glutamate transporters: spatio-temporal plasticity following hearing loss. Neuroscience. 2011; 178:218–239. [PubMed: 21211553]

Gassner HG, Shallop JK, Driscoll CL. Long-term clinical course and temporal bone histology after cochlear implantation. Cochlear Implants Int. 2005; 6:67–76. [PubMed: 18792320]

Henckaerts E, Linden RM. Adeno-associated virus: a key to the human genome? Future Virol. 2010; 5:555–574. [PubMed: 21212830]

Husseman J, Raphael Y. Gene therapy in the inner ear using adenovirus vectors. Adv Otorhinolaryngol. 2009; 66:37–51. [PubMed: 19494571]

Izumikawa M, Batts SA, Miyazawa T, Swiderski DL, Raphael Y. Response of the flat cochlear epithelium to forced expression of Atoh1. Hear Res. 2008; 240:52–56. [PubMed: 18430530]

Jero J, Mhatre AN, Tseng CJ, Stern RE, Coling DE, Goldstein JA, Hong K, Zheng WW, Hoque AT, Lalwani AK. Cochlear gene delivery through an intact round window membrane in mouse. Hum Gene Ther. 2001; 12:539–548. [PubMed: 11268286]

Kawamoto K, Ishimoto S, Minoda R, Brough DE, Raphael Y. Math1 gene transfer generates new cochlear hair cells in mature guinea pigs in vivo. J Neurosci. 2003; 23:4395–4400. [PubMed: 12805278]

Khan AM, Handzel O, Burgess BJ, Damian D, Eddington DK, Nadol JB Jr. Is word recognition correlated with the number of surviving spiral ganglion cells and electrode insertion depth in human subjects with cochlear implants? The Laryngoscope. 2005; 115:672–677. [PubMed: 15805879]

Konishi M, Kawamoto K, Izumikawa M, Kuriyama H, Yamashita T. Gene transfer into guinea pig cochlea using adeno-associated virus vectors. J Gene Med. 2008; 10:610–618. [PubMed: 18338819]

Kral A, O'Donoghue GM. Profound deafness in childhood. N Engl J Med. 2010; 363:1438–1450. [PubMed: 20925546]

Kujawa SG, Liberman MC. Adding insult to injury: cochlear nerve degeneration after "temporary" noise-induced hearing loss. The Journal of neuroscience : the official journal of the Society for Neuroscience. 2009; 29:14077–14085. [PubMed: 19906956]

Lawlor PA, Bland RJ, Mouravlev A, Young D, During MJ. Efficient gene delivery and selective transduction of glial cells in the mammalian brain by AAV serotypes isolated from nonhuman primates. Mol Ther. 2009; 17:1692–1702. [PubMed: 19638961]

Leake PA, Hradek GT, Hetherington AM, Stakhovskaya O. Brain-derived neurotrophic factor promotes cochlear spiral ganglion cell survival and function in deafened, developing cats. The Journal of comparative neurology. 2011; 519:1526–1545. [PubMed: 21452221]

Lee JH, Pradhan J, Maskey D, Park KS, Hong SH, Suh MW, Kim MJ, Ahn SC. Glutamate co-transmission from developing medial nucleus of the trapezoid body--lateral superior olive synapses is cochlear dependent in kanamycin-treated rats. Biochem Biophys Res Commun. 2011; 405:162–167. [PubMed: 21215254]

Lin HW, Furman AC, Kujawa SG, Liberman MC. Primary Neural Degeneration in the Guinea Pig Cochlea After Reversible Noise-Induced Threshold Shift. Journal of the Association for Research in Otolaryngology : JARO. 2011

Maeda Y, Sheffield AM, Smith RJ. Therapeutic regulation of gene expression in the inner ear using RNA interference. Adv Otorhinolaryngol. 2009; 66:13–36. [PubMed: 19494570]

Masuda M, Dulon D, Pak K, Mullen LM, Li Y, Erkman L, Ryan AF. Regulation of Pou4f3 gene expression in hair cells by 5' DNA in mice. Neuroscience. 2011

Noble W. Assessing binaural hearing: results using the speech, spatial and qualities of hearing scale. J Am Acad Audiol. 2010; 21:568–574. [PubMed: 21241644]

Obholzer N, Wolfson S, Trapani JG, Mo W, Nechiporuk A, Busch-Nentwich E, Seiler C, Sidi S, Sollner C, Duncan RN, et al. Vesicular glutamate transporter 3 is required for synaptic transmission in zebrafish hair cells. The Journal of neuroscience : the official journal of the Society for Neuroscience. 2008; 28:2110–2118. [PubMed: 18305245]

Petersen MB, Willems PJ. Non-syndromic, autosomal-recessive deafness. Clin Genet. 2006; 69:371–392. [PubMed: 16650073]

Praetorius M, Hsu C, Baker K, Brough DE, Plinkert P, Staecker H. Adenovector-mediated hair cell regeneration is affected by promoter type. Acta Otolaryngol. 2009:1–8. [PubMed: 19707904]

Roux I, Safieddine S, Nouvian R, Grati M, Simmler MC, Bahloul A, Perfettini I, Le Gall M, Rostaing P, Hamard G, et al. Otoferlin, defective in a human deafness form, is essential for exocytosis at the auditory ribbon synapse. Cell. 2006; 127:277–289. [PubMed: 17055430]

Ruel J, Emery S, Nouvian R, Bersot T, Amilhon B, Van Rybroek JM, Rebillard G, Lenoir M, Eybalin M, Delprat B, et al. Impairment of SLC17A8 encoding vesicular glutamate transporter-3, VGLUT3, underlies nonsyndromic deafness DFNA25 and inner hair cell dysfunction in null mice. Am J Hum Genet. 2008; 83:278–292. [PubMed: 18674745]

Seal RP, Akil O, Yi E, Weber CM, Grant L, Yoo J, Clause A, Kandler K, Noebels JL, Glowatzki E, et al. Sensorineural deafness and seizures in mice lacking vesicular glutamate transporter 3. Neuron. 2008; 57:263–275. [PubMed: 18215623]

Smith RJ, Bale JF Jr, White KR. Sensorineural hearing loss in children. Lancet. 2005; 365:879–890. [PubMed: 15752533]

Staecker H, Praetorius M, Baker K, Brough DE. Vestibular hair cell regeneration and restoration of balance function induced by math1 gene transfer. Otol Neurotol. 2007; 28:223–231. [PubMed: 17255891]

Steven Colburn H, Shinn-Cunningham B, Kidd G Jr, Durlach N. The perceptual consequences of binaural hearing. Int J Audiol. 2006; 45(Suppl 1):S34–S44. [PubMed: 16938773]

Takamori S, Malherbe P, Broger C, Jahn R. Molecular cloning and functional characterization of human vesicular glutamate transporter 3. EMBO Rep. 2002; 3:798–803. [PubMed: 12151341]

von Ilberg CA, Baumann U, Kiefer J, Tillein J, Adunka OF. Electric-acoustic stimulation of the auditory system: a review of the first decade. Audiology & neuro-otology. 2011; 16(Suppl 2):1–30. [PubMed: 21606646]

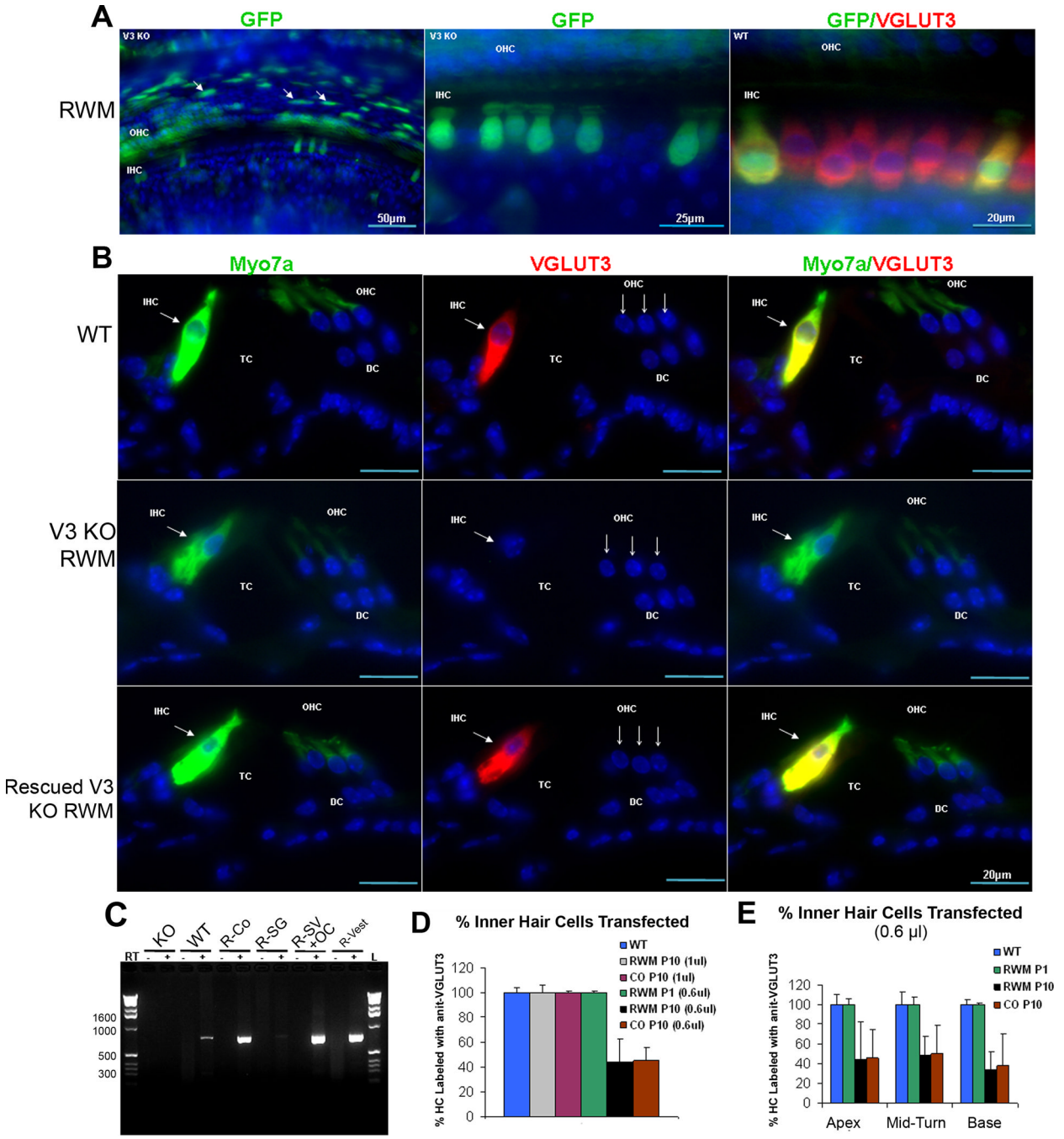

Figure 1. AAV1-GFP transduction in mice organ of Corti

1A. AAV1-GFP was used to assess viral delivery to the cochlea on organ of Corti surface preparations. AAV1 transfects a number of cell types including inner (IHC) and supporting cells (white arrows, left panel) in the organ of Corti. The VGLUT3 KO (V3KO, 1A middle panel) documents IHC labeling of transfected cells only. In the WT mouse (1A right panel), VGLUT3 co-labels IHCs (red) along AAV1- GFP transfected cells (green). 1B. VGLUT3 expression following AAV1-VGLUT3 delivery via the RWM, delivered at P10-12, and stained with anti-myosin 7A antibody (green, used as a hair cell marker, left column), anti-VGLUT3 antibody (red, middle column) and merged (right column). WT mice show IHCs labeled with both anti-Myo7A and VGLUT3 as expected (1B upper right panel) whereas

KO mice only show Myo7a expression (1B middle right panel). Following AAV1-VGLUT3 delivery, the IHC is co-labeled by both anti-Myo7a and anti-VGLUT3 antibodies (1B lower right panel) (TC=tunnel of Corti, DC=Deiter‘s cells, OHC=outer hair cells, IHC=inner hair cells). 1C. RT-PCR was used to verify VGLUT3 mRNA expression in the transfected, KO (first lane) and WT (2nd lane) mice. Rescued whole cochlear extract (R-Co) demonstrates strong VGLUT3 mRNA expression, as does the stria vascularis + organ of Corti lane (R-SV +OC) and vestibular neuroepithelium (R-Vest). Spiral ganglion only shows weak mRNA expression (R-SG). 1D-E. Inner hair cells labeled with anti-VGLUT3 antibody following transfection were counted, tabulating both the entire cochlea and within the base, mid-turn and apex to determine differences in regions (at P10-12 delivery-WT n=5, CO n=5, RWM n=6 and at P1-3 delivery, RWM n=6). At P10-12, when 1μl of virus was microinjected, 100% of IHCs were labeled similar results were seen at P1-3 viral delivery (1D) when injected with 0.6 μl. In contrast, when 0.6μl of virus was injected at P10-12, approximately 40% of IHCs were labeled, with no significant differences seen between the apex, mid-turn, or base in the variability of IHC labeling with the delivery technique (1E).

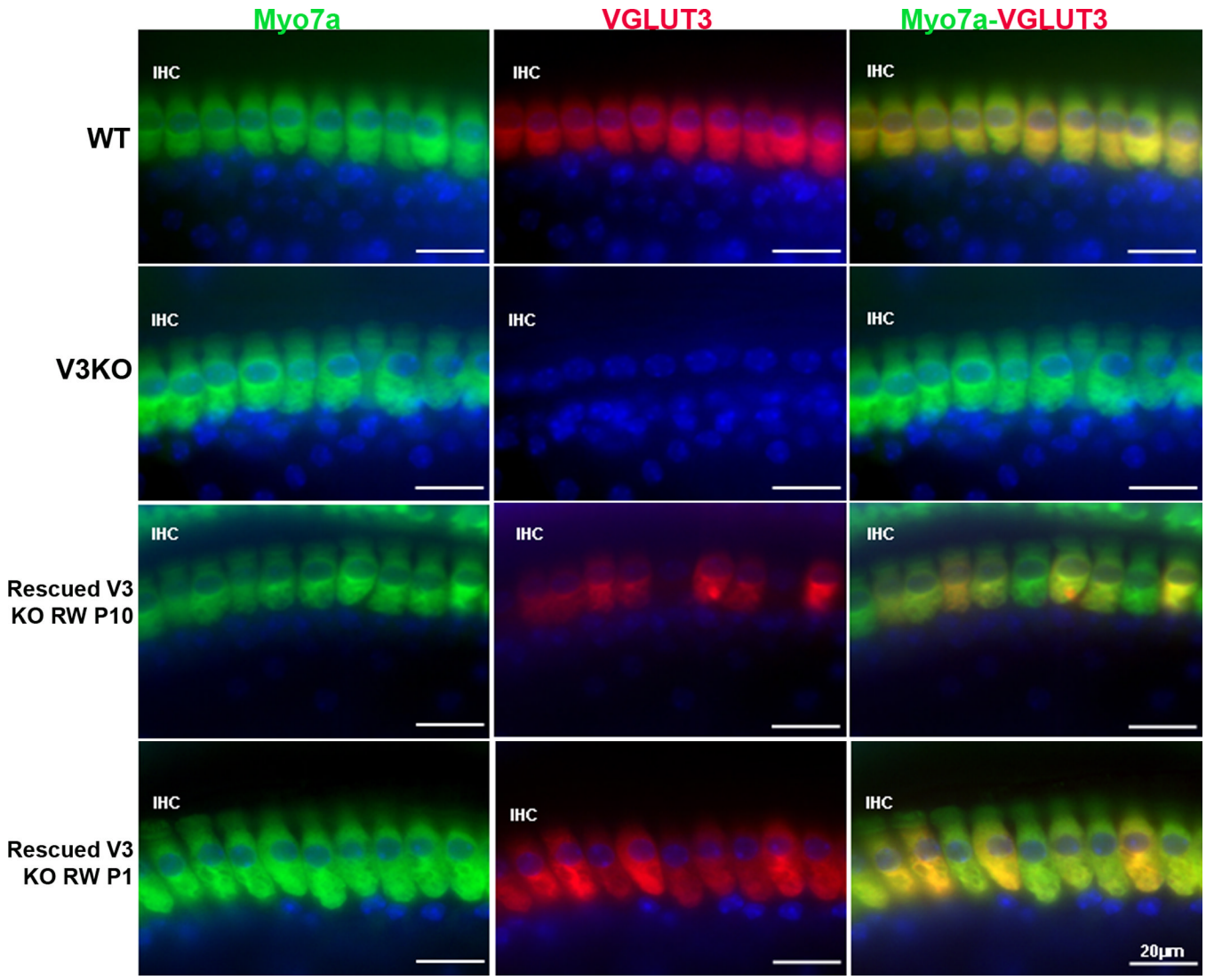

Figure 2. VGLUT3 IHC Transfection: Early vs Late Delivery

AAV1-VGLUT3 delivery at P1-3 vs P10-12 are compared using similar amount of virus (0.6 µl), and examined at ~P30. Anti-Myo7a antibody (green), and anti-VGLUT3 antibody (red) are used for staining, and the merged images (yellow). As expected, IHC from WT mice show both anti-Myo7a and anti-VGLUT3 staining (row 1) whereas KO mice only show anti-Myo7a label (row 2). Delivery of virus via the RWM at P10-12 results in fewer IHCs expressing VGLUT3 (row 3), whereas similar doses of virus injected at P1-3 results in 100% of hair cells transfected in all animals (row 4), (TC=tunnel of Corti, DC=Deiter‘s cells, OHC=outer hair cells, IHC=inner hair cells).

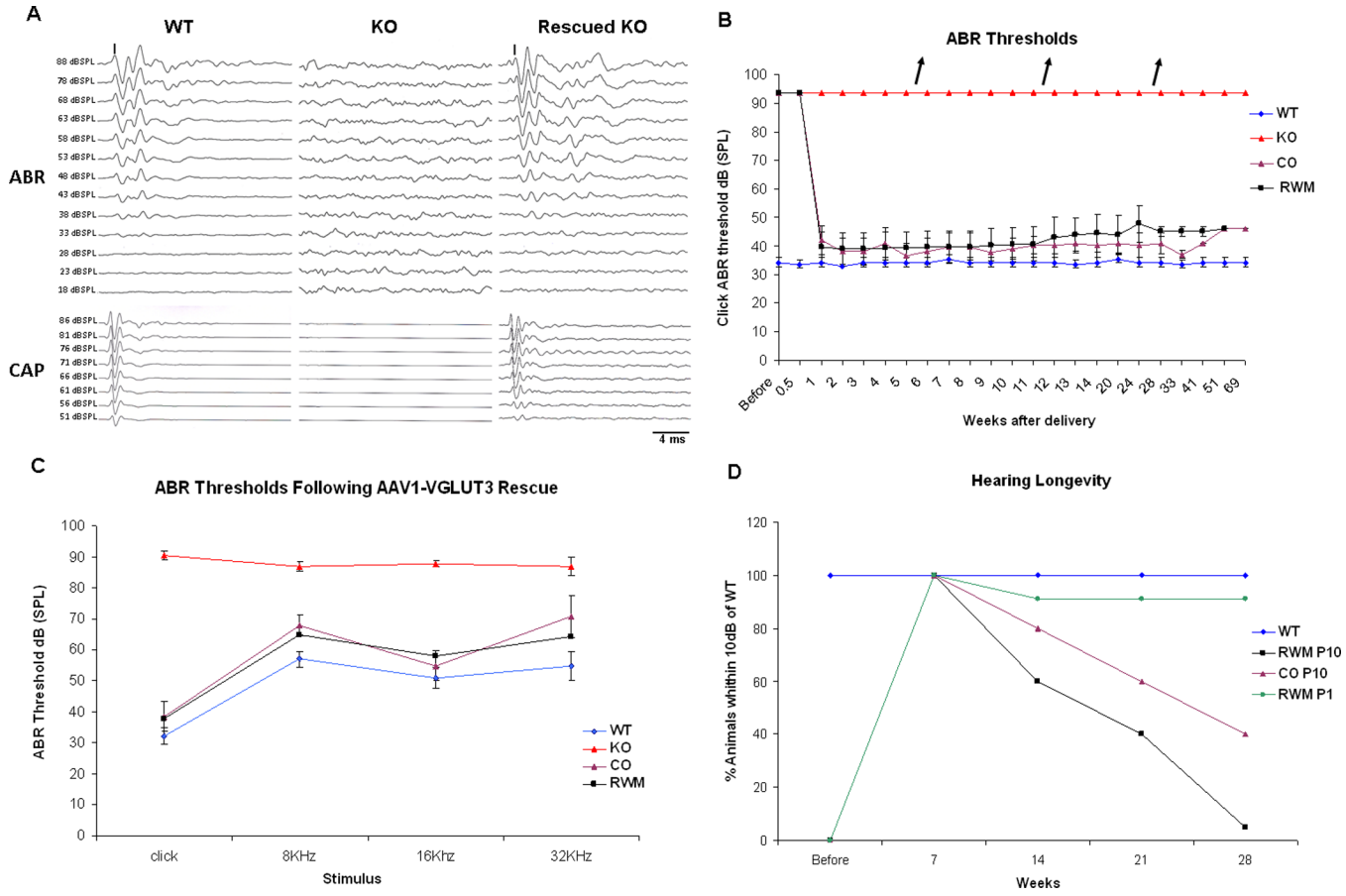

Figure 3. Hearing Restoration in the VGLUT3 KO Mice

3A. Representative ABR and CAP tracings from WT, KO and rescued KO mice following delivery of 0.6μl AAV1-VGLUT3. Waveforms from the WT and rescued mice appear similar while KO mice show no ABR and no CAP responses. "I" indicates the location of ABR wave I. 3B. Rescued mice begin to show hearing recovery within 7 days post-delivery (P17-19), with near normalization of ABR thresholds by 14 days post-delivery (P24-26). Hearing recovery is seen with both CO and RWM delivery through 69 weeks. Black arrows in figure 3B indicate absence of ABR threshold of the KO above 92 dB (*the maximum level that our recording equipment can measure*). 3C. At 40 days post-delivery (P50-52), similar levels of recovery are noted at 8 and 16 kHz, while at 32 kHz, CO delivery appears to result in slightly elevated thresholds, though still significantly better than KO. 3D. Hearing longevity, as defined as the number of mice with ABR threshold levels within 10db of WT levels at each time point, is measured for RWM at P10-12, CO at P10-12 and RWM at P1-3. For viral delivery at P10-12, CO delivery results in longer-lasting hearing recovery on average than RWM delivery, with some rescued KO in each group maintaining ABR thresholds to within 10db of WT animals beyond 28 weeks. However, 100% of rescued KO with RWM delivery recover hearing while only 17% of CO-rescued mice recover hearing. The number of animals with viral delivery at P10-12 at each time point is the following: RWM 0–9 weeks n=19, 10–13 weeks n=12, 14–24 weeks n=8, 24–28 weeks n=1, 28+ weeks n=1; CO 0–7 weeks n=5, 8–14 weeks n=4, 15–20 weeks n=3, 21–28 weeks n=2, 28+ weeks n=1). In contrast, in mice undergoing viral delivery at P1-3, all animals maintain ABR threshold recovery at least through 9 months (n=5).

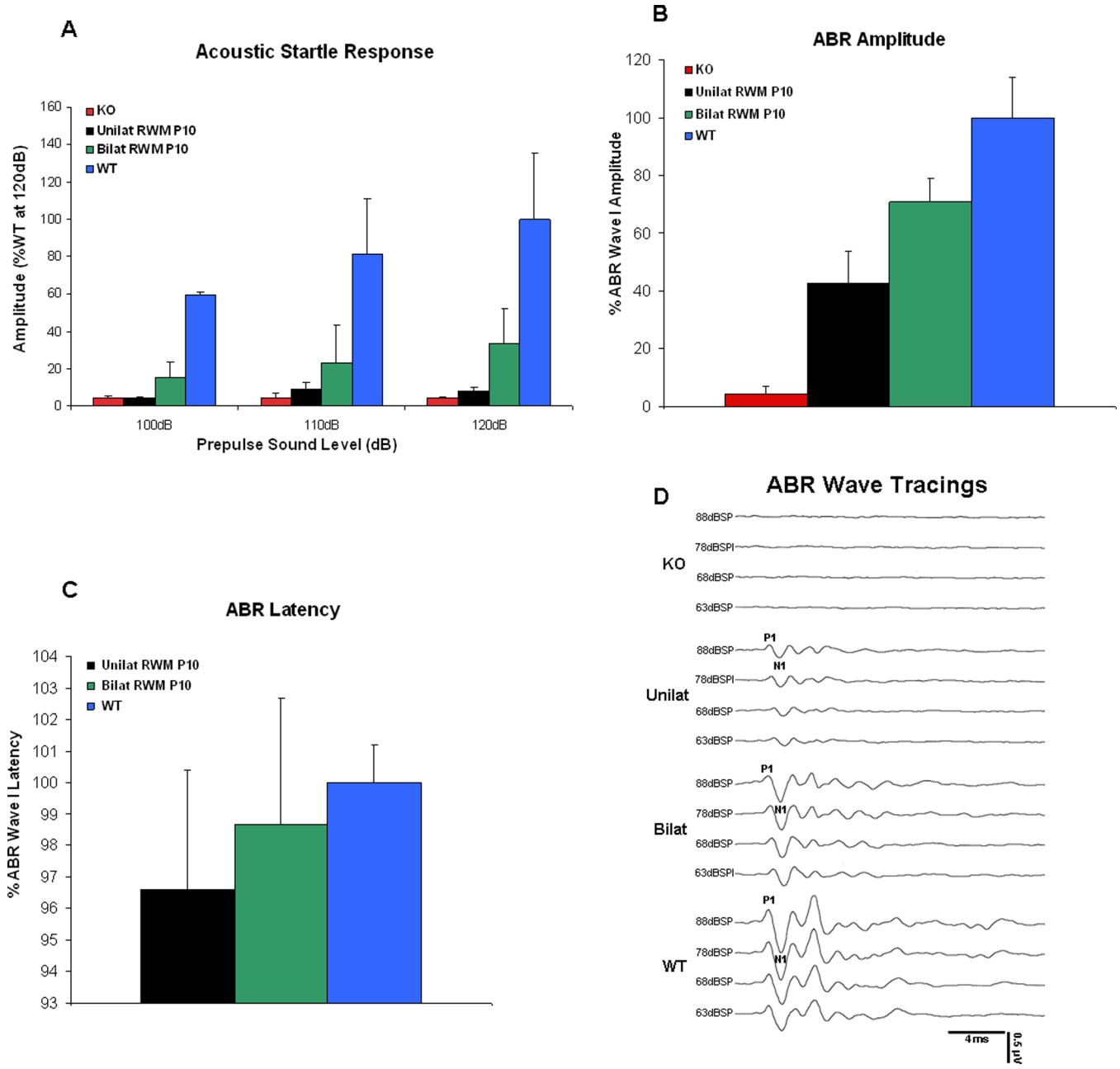

Figure 4. Behavioral Measures and Physiologic Growth Following AAV1-VGLUT3 Rescue

4A. Startle responses were studied as an additional behavioral measure of hearing recovery 3 weeks following viral delivery (P31-33). While none of the rescued mice recover startle responses to WT levels, they nonetheless develop a response, which increases when both ears are rescued; the louder the sound delivered (100, 110, and 120db presentation levels), the more robust the startle response, with rescue of both ears (Bilat) creating a larger response than a single ear (Unilat). These differences were statistically significant. 4B. Similar growth was seen for ABR wave I amplitudes when both ears (Bilat) as compared to a single ear (Unilat) were rescued, though again, not as robust as in the WT mice. 4C. ABR wave I latency was measured, which showed no statistically significant differences between unilateral, bilateral, rescued mice and WT, though there was a trend towards an increased

latency in the rescued compared to WT mice. 4D. Representative ABR tracings documenting increasing wave I amplitudes from the KO, unilaterally rescued KO (Unilat), bilaterally rescued KO (Bilat) and WT mice.

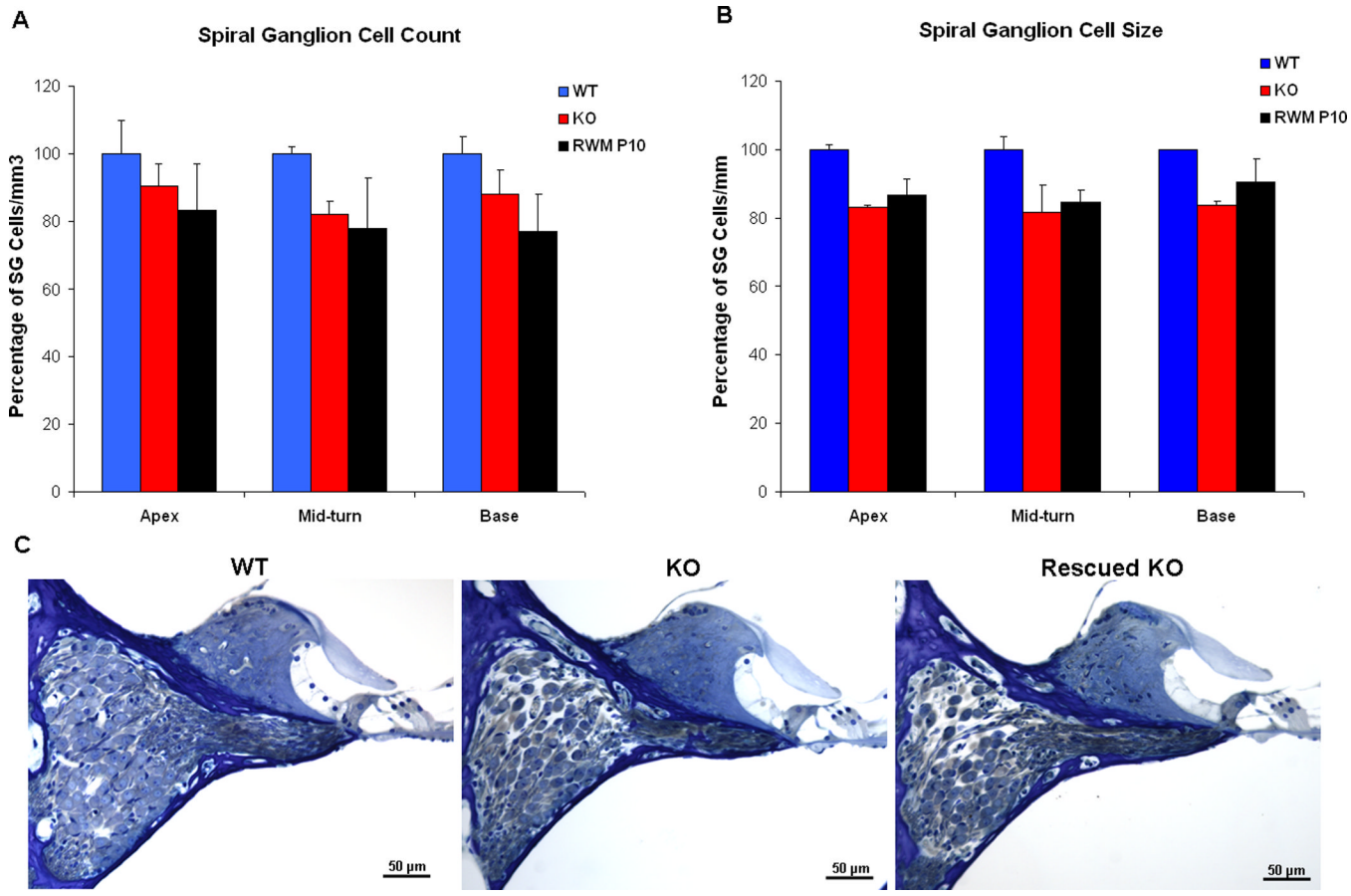

Figure 5. Spiral Ganglion Cell Counts

In these studies the AAV1-VGLUT3 delivery was done at P10-12 and at P1-3. Spiral ganglion (SG) cell counts in rescued mice vs. KO and WT mice were undertaken at P21 (5A-B) and at P5mo (data not shown) for P10-12 virus delivery, and P2mo (data not shown) for P1-3 virus delivery. AAV1-VGLUT3 transfection did not result in a reversal of the SG neuronal loss in either age group. No significant differences were seen between the groups. These results also document the lack of trauma (5C) associated with virally-mediated delivery of VGLUT3 through the RWM, with normal organ of Corti morphology, including inner- and out-hair cells, spiral ganglion neurons and stria vascularis (data not shown)

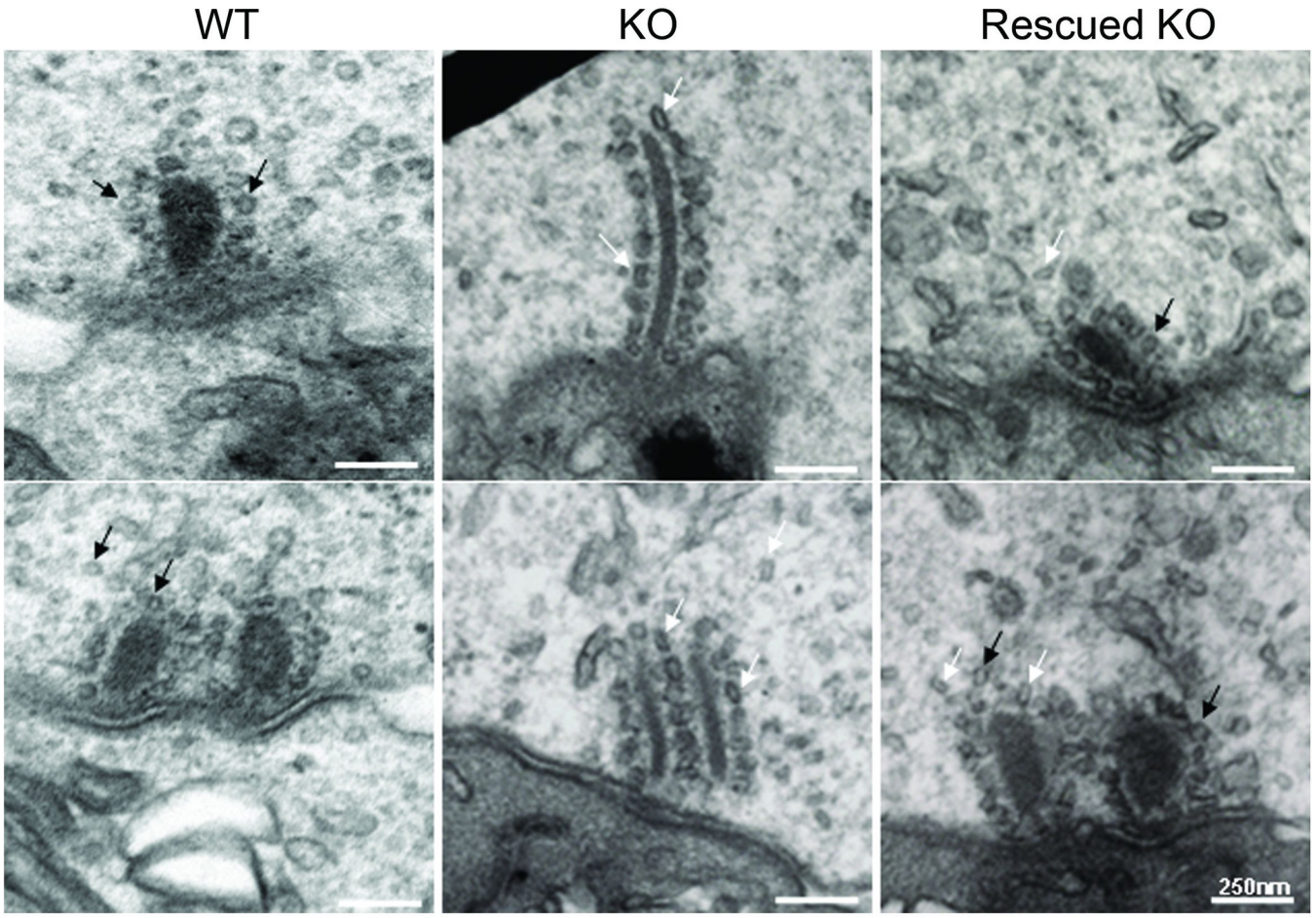

Figure 6. Partial Normalization of Synaptic Ribbon Morphology in the Rescued Mice

Electron microscopy was performed on broken serial thin sections of the synaptic region of the IHCs which were cut in a horizontal plane parallel to the basilar membrane in the same orientation for the WT, KO and rescued KO mice. As previously reported (Seal et al., 2008), VGLUT3 KO mice demonstrate abnormally thin, elongated ribbons in IHC synapses (middle column), as compared to WT littermates (left column). In the rescued mice (right column, single ribbon shown on top, double on the bottom), ribbon synapses are normal appearing, taking on a more rounded shape similar to the WT. Black arrows point to the normal or circular synaptic vesicles and white arrows point elongated synaptic vesicles.

Table 1
Transmission Electron Micrographic Analysis of the Ribbon Synapse

This analysis compares the ribbon synapse and vesicles in WT vs. KO vs. AAV1-VGLUT3 rescued KO mice. Electron microscopy was performed on broken serial thin sections of the synaptic region of the IHCs which were cut in a horizontal plane parallel to the basilar membrane with identical handling and orientation for the WT, KO and rescued KO. When differentiating vesicles as either “circular” or “elongated”, a vesicle was defined as ‘circular’ when the perpendicular diameters were found to within 50% of each other. Any vesicle with unequal perpendicular dimensions (>50% difference) was counted as ‘elongated,’ and any ribbon synaptic body that had a length greater than three times its greatest width was considered to be ‘abnormal’ in appearance.

	WT	KO	Rescued KO
Number of inner hair cells examined	58	50	61
Total number of ribbons	18	20	18
Number of floating ribbons	3	3	4
Number of normal ribbons	18	0	17
Number of elongated ribbons	0	20	1
Ave # of synaptic vesicles associated w/ the ribbon	14.44 ± 1.92	16.26 ± 2.85	19.17 ± 4.52
Shape of the synaptic vesicles	All circular	All elongated	Mixture of circular + elongated
Average number of docked synaptic vesicles	2.28 ± 1.27	1.56 ± 0.92	2 ± 0.84